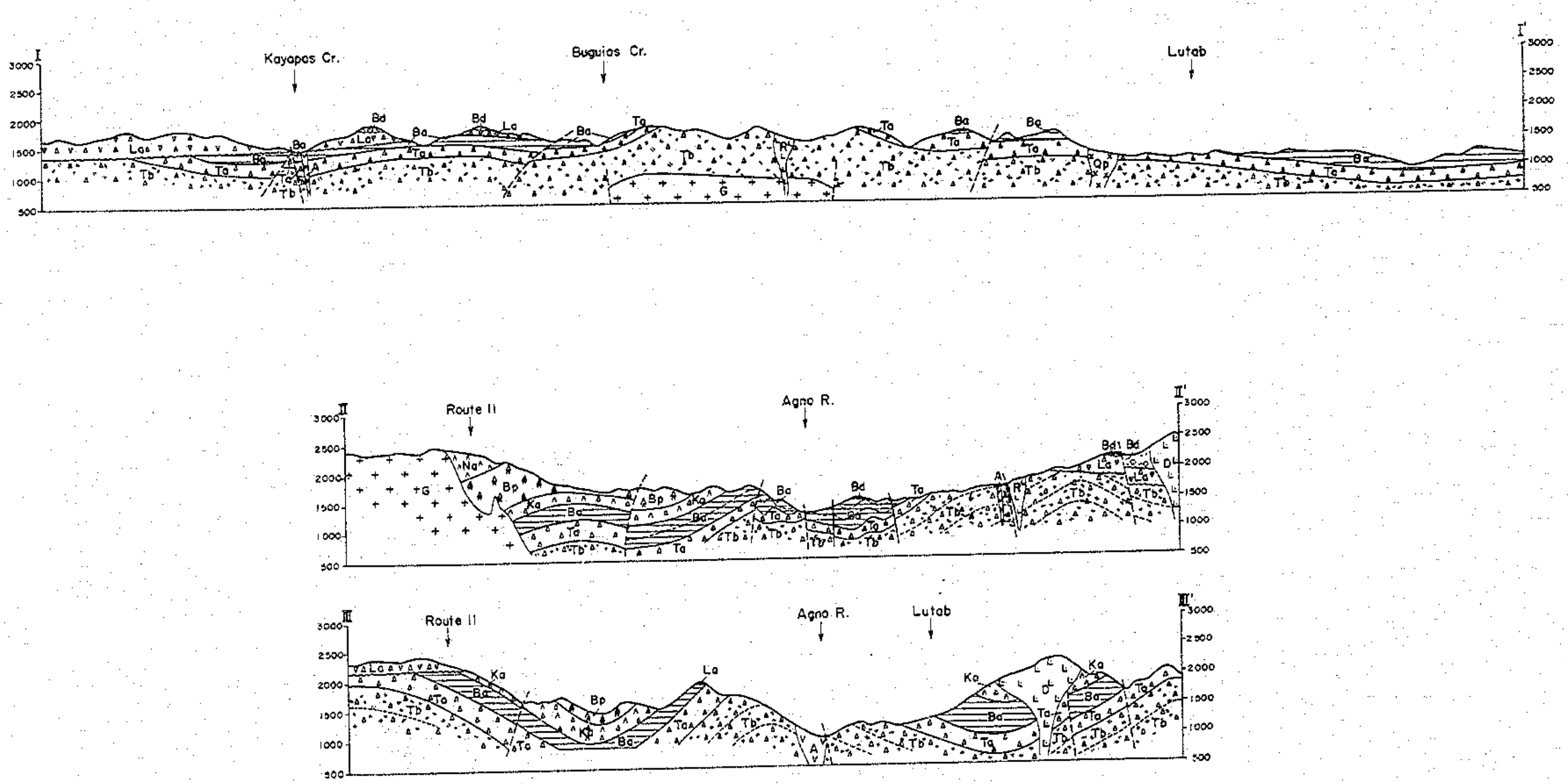

Geological Profiles of Fig. II–1–7

possibly to be of lower Miocene (Table II–1–4, II–1–5),

The formation is similar to the rock facies of Oligocene to Miocene pyroclastics and the sediments prevailing in the southern part of Daklan area are correlated to the Zigzag formation in the Baguio district. This formation is classified from lower to upper into six (6) groups, that is:

1) Kayapas creek pillow lava member
2) Toking creek basaltic and andesitic volcanics member
3) Buguias creek alternation member
4) Kagosit andesitic volcanic member
5) Batan river pillow lava member
6) Nanayegan creek andesite member

1) Kayapas creek pillow lava member

Type locality : Kayapas creek, upper portion of Buguias Central

Thickness : 300 m

Lithology : This member consists of basaltic pillow lava (Fig. II–1–8). Pillow structure is well developed at the upper stream of Kayapas creek with 20 cm to 1 meter diameter pillow forms. Composition of the rock is basaltic with 2–3 mm of pyroxene phenocrysts and the interspaces between pillow structure is filled with calcite, chlorite and epidote. The pillow structure indicates a strike of N20E and dip of 20N.

The contact of lower portion of the member is bounded by a fault to granodiorite.

2) Toking creek basaltic and andesitic volcanic member

Type locality : Upper stream of Toking creek at the northern part of Buguias Central. The member is distributed along Toking creek at the eastern part of Buguias and along the Agno river from Buguias creek to Lutab and Kabayan.

Thickness : 1,200 m

Lithology : The formation is mainly composed of andesitic and basaltic lava, pillow lava and coarse to fine pyroclastic materials with significant limestone lenses. At the northern part of Buguias Central, basaltic pyroclastics, pillow lava, hyaloclastite (Fig. II–1–9a) and andesitic lava and tuff breccia were found. The lower part of the formation is bounded by a fault in contact with the pyroclastics of Loo formation.

Basaltic pyroclastics and hyaloclastite include basaltic breccia, rhyo-dacite and limestone. Brecciated basalt lava, 5 cm to 50 cm size, is coated with calcite and chlorite.

The pillow form of andesite lava is not well developed, and is purplish to dark green in color. Mafic minerals are mainly olivine and pyroxene. Basaltic pillow lava with calcareous amygdal shows well developed pillow form, 30 cm to 1 m in diameter.

Along Buguias creek, the member is mainly composed of basaltic tuff breccia and hyaloclastite. However, at Lutab and Kabayan area along the Agno and its tribataries the member consists of andesitic to basaltic pyroclastics, well graded fine tuff, alternation of sheets of lenticular limestone (Fig. II–1–10), rhyolite lava and pyroclastics. Rhyolite lava rock facies changes from massive with developed joints to brecciated lava and tuff breccia with accidental pebbles. Pumiceous tuff associated with rhyolitic activity includes limestone breccia and is pale green in color.

As stated above, this member of the formation is mainly composed of basaltic and andesitic tuff breccias and hyaloclastite. In the southern part of the formation, basalt lava interbedded with well developed coarse to fine tuff while acidic volcanics are observed at the central part. The geological structure of the formation shows N-S trend strike at the north and south of the area, forming the anticlinal axes. However, the strike of the formation at the central part changes to E-W trend, forming an up-lifted structure.

A concordant relationship between Kayapas pillow lava and this member was established.

Microscopic observation ; augite olivine basalt (Sample No. N–55) (Fig. II–1–9b)

Phenocryst ; plagioclase · olivine · augite · opaque mineral

Plagioclase phenocrysts are predominant, commonly 0.3 ~ 1.0 mm long and they are represented by albite and montmorillonite in parts.

Olivine phenocrysts are commonly 0.5 ~ 2.0 mm long and they are replaced by iddingsite wholly and/or partly along cleavages. They are rich in forsterite component. Augite phenocrysts are 0.3 ~ 0.6 mm long and opaque minerals are 0.1 ~ 0.3 mm long.

Table II–1–4 Smaller Foraminifera

No. 1	M–22	No foraminifera		
No. 2	M–60	〃		
No. 3	M–101	〃		
No. 4	N–38	〃		
No. 5	N–48	〃		
No. 6	N–84	〃		
No. 7	N–94	Nonion sp.	4	1 Benthonic Foram are observed without Planktonic *Foram.* The stage is not sure but it would be regarded as Middle Miocene.
		Gyroidina sp.	5	
		Cal. Foram. gen. and sp. indet	10	
No. 8	N–98a	Globigerinodes sp.	4	2 These sedinent is considered to be deposited in a open sea so that only Planktonic Foram is observed in them. The stage is not sure but it would be regarded as Lower Miocene.
		Globigerine sp.	3	
		Pla. Foram. gen. and sp. indet	10	
No. 9	N–98B	Cla. Foram. gen. and sp. indet	5	
No. 10	N–116	No. Foraminifera		
No. 11	N–129	Globigerinoides sp.	25	Same as 2
		Globigerine sp.	10	
		Pla. Foram. gen. and sp. indet	8	
No. 12	N–176	No Foraminifera		
No. 13	N–177	〃		

Table II–1–5 Result of Fission Track Age

Sample No. N–112

Grain		Track of spontaneous nuclear fission		Track of inductive nuclear fission		$\rho s/\rho i$	Age T ($X10^6$ y)
		Ns / lattic **	$\rho s(cm^{-2})$	2 Ni / lattic	$\rho i\ (cm^{-2})$		
1		52 / 50	3.76×10^6	147 / 50	1.07×10^7	3.51×10^{-1}	25.6
2		61 / 50	4.43×10^6	138 / 50	1.00×10^7	4.43×10^{-1}	32.3
3		/	too many	/			–
4		/	do	/			–
5		/		/			–
6		/	too many	/			–
7		88 / 100	3.19×10^6	340 / 100	1.23×10^7	2.59×10^{-1}	18.9
8		56 / 50	4.07×10^6	96 / 50	6.90×10^6	5.90×10^{-1}	43.0
9		123 / 200	2.23×10^6	420 / 200	7.60×10^6	2.93×10^{-1}	21.3
10		25 / 25	3.63×10^6	60 / 25	8.71×10^6	4.17×10^{-1}	30.4
11		/		/			
Total	A						1 28.6
	B						2 A/B

Sample No. N–125

Grain		Track of spontaneous nuclear fission		Track of inductive nuclear fission		$\rho s/\rho i$	Age T ($X10^6$ y)
		Nx / Lattic **	$\rho s(cm^{-2})$	2 Ni / lattic	$\rho i\ (cm^{-2})$		
1		1 / 700	0.52×10^4	1030 / Ns	5.34×10^6	0.97×10^{-3}	0.07
2		0 / 800	–	970 /	4.40×10^6	–	–
3		0 / 350	–	482 /	5.00×10^6	–	–
4		0 / 450	–	494 / 300	5.97×10^6	–	–
5		2 / 400	1.81×10^4	334 / 400	3.03×10^6	5.99×10^{-3}	0.44
6		0 / 400	–	390 / 400	3.54×10^6	–	–
7		3 / 400	2.72×10^4	500 / 400	4.54×10^6	5.99×10^{-3}	0.44
8		0 / 250	–	250 / 400	2.27×10^6	–	–
9		0 / 600	–	802 / 400	7.27×10^6	–	–
10		0 / 450	–	440 / 400	3.99×10^6	–	–
11		0 / 450	–	572 / 300	6.92×10^6	–	–
12		0 / 400	–	412 / 300	4.98×10^6	–	–
13		0 / 425	–	788 / 400	7.15×10^6	–	–
14		0 / 150	–	250 / 200	4.54×10^6	–	–
15		0 / 425	–	524 / 400	4.75×10^6	–	–
16		0 / 250	–	402 / Ns	5.83×10^6	–	–
17		0 / 200	–	240 /	4.35×10^6	–	–
18		0 / 175	–	300 / 200	5.44×10^6	–	–
19		0 / 200	–	338 / Ns	6.13×10^6	–	–
20		0 / 100	–	150 /	5.44×10^6	–	–
21		0 / 100	–	178 /	6.46×10^6	–	–
22		0 / 150	–	200 /	4.84×10^6	–	–
Total	A						1
	B	6 / 7825	2.78×10^3	10046/7350	7.96×10^6	5.60×10^{-4}	2 A/B 0.04

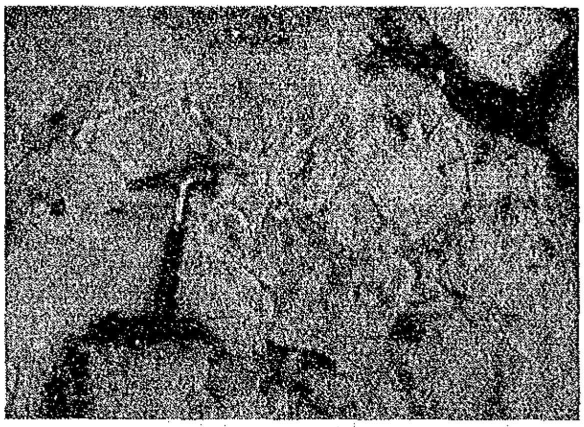

Fig. II–1–8 Photograph
(basaltic pillow lava, Kayapas cr. pillow lava member Buguias formation, at Kayapas Creek)

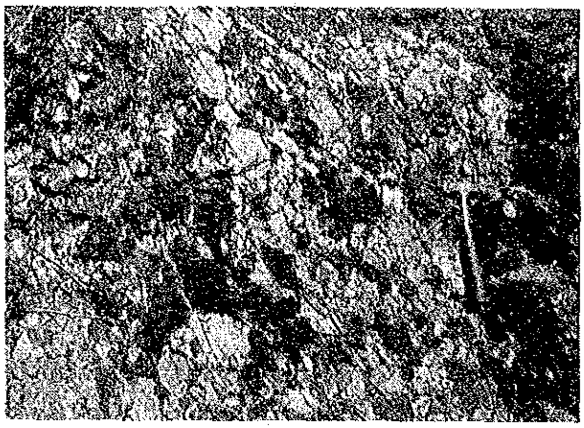

Fig. II–1–9a Photograph
(basaltic hyaloclastite cemented with calcareous material, Toking cr. basaltic and andesitic volcanics member, Buguias formation at Toking Creek)
(Sample no. N–55)

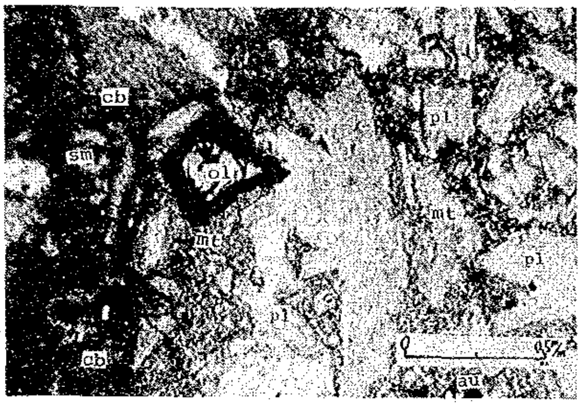

Fig. II–1–9b Microscopic Photograph of Sample no. N–55.
augite-olivine basalt and carbonate material

pl ; plagioclase
ol ; olivine
au ; augite
mt ; montmorillonite
cb ; carbonate material
sm ; smaller foraminifera

(open nicol)

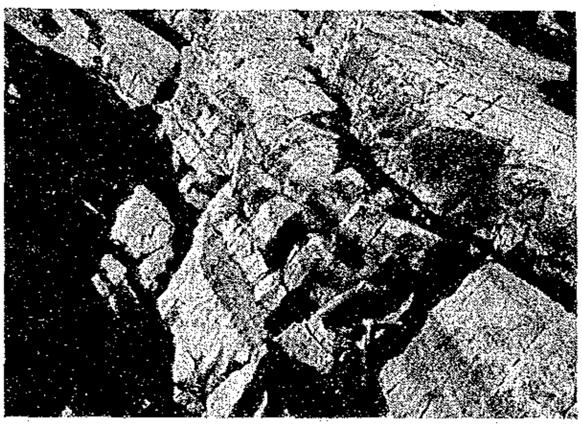

Fig. II–1–10 Photograph
(alternative lime stone Toking cr. basaltic and andesitic volcanics member, Buguias formation, at a southern small creek of Buguias cr.)

Groundmass ; This is replaced by secondary minerals perfectly. Secondary minerals are composed of predominant montmorillonite and carbonate minerals. The texture represents amygdaloidal, filled with analcite and carbonate minerals, and hyaloclastite cemented with foraminiferous carbonate.

3) Buguias creek alternation member

Type locality : Lower portion of Buguias creek in the southern part of Buguias Central. The formation is distributed from Bugias to Kayapas creek along the Agno river and Kabayan to the eastern slope of Batan river with a belt-like form.

Thickness : 350 m

Lithology : The member is mainly composed of finetuff, muddy tuff and mudstone associated with andesitic pyroclastic rocks and lapilli tuff with small accounts of limestone (Fig. II–1–11a). Fine tuff at the type locality, is well graded, with a thickness of 10 cm to 50 cm, and is well developed with rhythmic banding of alternating medium to fine grained tuff, light gray to pale-green in color. The member has 200 to 500 meters series of folding structures exhibiting N-S trend axes. At the Buguias area, poorly solicified alternation of coarse to fine tuff is often intercalated with andesitic pyroclastic rocks. This member of the formation at Kayapas creek and its branch consists of tuff breccia, lapilli tuff, and alternation of coarse to fine tuff. The bed is 0.5 to 1 m thick and includes large amounts of accidental breccias such as andesite, subangular to subrounded rhyolite, mudstone and limestone. The lower part of the member consists of pumiceous tuff and limestone. The pumice in the bed becomes flat in shape with 1 to 5 cm in diameter and is chloritized exhibiting a pale green color. Matrix of the rock is calcareous associated with 0.5 to 1 cm of pumiceous material. Fossils are scarce in the bed.

This member of the formation at the Agno river and lower portion of Toking creek consists of andesitic tuff breccia and lapilli tuff intercalated with limestone. Many of the sand pipe shaped trace fossils are observed in the alternation of lapilli tuff and limestone. Slumping structure is also observed with well developed slump fold. (Fig. II–1–12a)

Andesitic tuff breccia and lapilli tuff are predominant in this member and are pale green in color and are well graded. Limestone is massive with light grayish color and contains shell fragments and foraminiferas.

At Kabayan along the Agno river and its tributaries, alternation of well graded andesitic and basaltic pyroclastics include angular to subangular breccias of andesite and basalt. It also contains a number of mudstone and limestone as accidental materials.

The rock facies of this member changes from the northern part of Buguias to the southern part of Kabayan. At the north, this member mainly consists of fine grained pyroclastics and the bed is comparatively thin and is slightly silicified.

At the south, on the other hand, this member is mainly composed of alternation of coarse pyroclastics, intercalated conglomerate, tuff breccia and lapilli tuff. The bed is rather thicker than that of northern part. Furthermore, a number of metavolcanic breccia presumably from the basement rock is included. The structure of this member generally shows a N-S trend strike and complicated folding with gentle to steep dips. A very intense deformation caused by faulting and a series of small scale folding structure with N-S trend axes were observed.

Foraminifera is found in limestone and mudstone from this member. However, the depositional age could not be determined from the fossil.

The relationship with the lower member of Toking creek basaltic and andesitic volcanics is concordant.

Microscopic observation ; accidental lapilli tuff (Sample No. N–135) (Fig. II–1–11b)

Lapillies are composed of altered amygdaloidal basalt, altered andesite and limestone.

Matrix are highly altered to montmorillonite, chlorite and carbonate minerals.

Limy mudstone ; (Sample No. N–128) (Fig. II–1–12b)

This rock is consisting of many smaller foraminiferas.

4) Kagosit andesitic volcanic member

Type locality : Adut creek, south of Kabayan

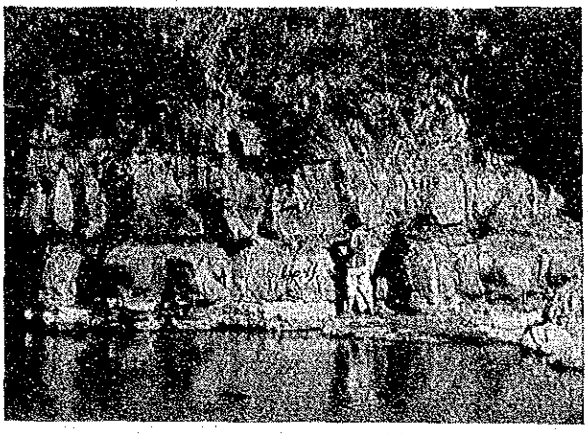

Fig. II–1–11a Photograph
(alternation of lapilli tuff and mudstone, Buguias cr. alternative member, Buguias formation, at Buguias)
Sample no. N–135

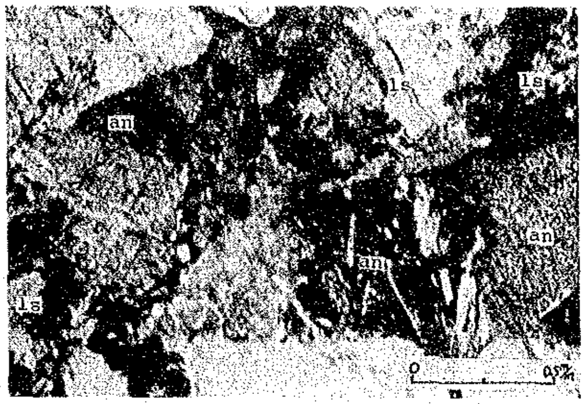

Fig. II–1–11b Microscopic Photograph of Sample no. N–135,
accidental lapilli tuff composed of andesite and calcareous lapilli

an ; andesite
ls ; limestone

(open nicol)

Fig. II–1–12a Photograph
(slump structure of mudstone in Buguias cr. alternative member at Buguias)

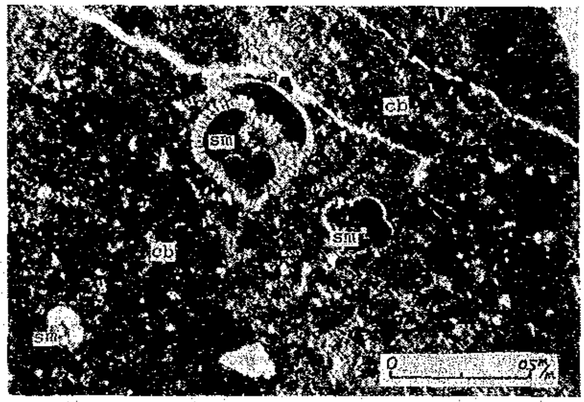

Fig. II–1–12b Microscopic Photograph of Sample no. N–128,
calcareous mudstone (small foraminifera bearing), Buguias cr. alternative member, Buguias formation

sm ; small foraminifera
cb ; carbonate material and muddy material

(cross nicol)

This member if exposed from Kagosit to Batan river on a limb of an anticline trending N-S and also distributes from Pulibo ridge to Lungaw with N-S direction.

Thickness : 350 m

Lithology : This member is mainly composed of andesitic tuff breccia and hyaloclastite (Fig. II–1–13a) intercalated with brecciated lava and pumice tuff. At the type locality, greenish and massive andesitic tuff breccia was deposited on the Buguias creek alternative member. The breccia included in this member is of essential materials with 5 to 20 cm in diameter. The upper part of the member intercalates with pumiceous lapilli tuff, which is chloritized and shows a pale green color. Lapilli tuff contains accidental materials of limestone. Andesitic hyaloclastite, tuff breccia and coarse pyroclastics are observed at Boloc along the Agno river. Hyaloclastite is dark green and massive with amygdules of calcite.

The relationship with Buguias creek alternation member is concordant.

Microscopic observation ; augite andesite (Sample No. N–95) (Fig. II–1–13b)

Phenocryst ; plagioclase · augite

Plagioclase phenocrysts are 1.0 ~ 4.0 mm long. They are shown worm-eaten texture to be replaced by albite, carbonate and montmorillonite in same parts.

Groundmass ; The groundmass is cryptcrystalline and occures carbonate stringers.

5) Batan river pillow lava member

Type locality : Upper stream of Batan river.

This member is distributed at the middle stream of Adut river and from Batan river to Mt. Mungeote along the wing of N-S trending anticlinal axes, and is also exposed from Nabolicon creek to Sinepsip along the wing of N-S trending synclinal axes.

Thickness : 300 m±

Lithology : The member is mainly composed of basaltic pillow lava (Fig. II–1–14a) intercalated with basaltic tuff, andesitic pillow lava and its pyroclastics. The size of pillow ranges from 20 cm to 1 m and are dark green to dark purple in color. Interspaces between pillows are filled with chlorite and secondary epidote. The phenocrysts of the rock are pyroxene. Pyroclastic rock is well graded tuff breccia and fine tuff, which shows parallel laminations.

The differences of rock facies and occurrences between this member and Kayapas creek pillow lava are not observed.

The Kagosit andesitic volcanic member is concordant to Batan river pillow lava member.

Microscopic observation ; olivine basalt (Sample No. N–96) (Fig. II–1–14b)

Phenocryst ; plagioclase · olivine

Plagioclase phenocrysts are 0.4 ~ 0.7 mm long and they are represented worm-eaten texture to be replaced by montmorillonite and albite. Olivine phenocrysts are 1.0 ~ 2.0 mm long and they are replaced by epidote in parts.

Groundmass ; glass · plagioclase · secondary minerals

The groundmass are shown amygdaloidal texture filled by montmorillonite and zeolite etc..

6) Nanayegan creek andesite member

Type locality : Nanayegan creek north of Natubleng, western part of survey area.

Thickness : 400 m±

Lithology : This member is the uppermost of Buguias formation and consists mainly of andesite lava and brecciated lava intercalated with pumice tuff. At the type locality, the andesite contains pyroxene as phenocryst and is characterized by well developed columnar joint. Pumice or pumice tuff is altered to montmorillonite showing a green color. (Fig. II–1–15)

Nanayegan member is concordant with Batan pillow member.

1–4–2 Loo Formation

Type locality : Loo area

The formation is exposed at the northern part of survey area.

Thickness : Maximum 800 m

Lithology : The formation consists mainly of andesite, dacite and pyroclastics. At type locality along the Agno river and its tributaries, andesitic volcanic conglomerate, tuff breccia and pyroclastics are developed. Volcanic conglomerate is mainly composed of andesitic conglomerate with angular to subangular andesite, basalt and granodiorite as accidental

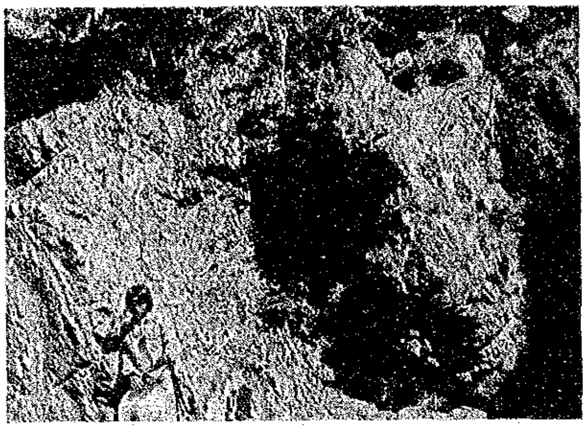

Fig. II–1–13a Photograph
(hyaloclastite of glassy andesite,
Kagosit andesitic volcanic member,
Buguias formation at Agno river)
Sample no. N–95

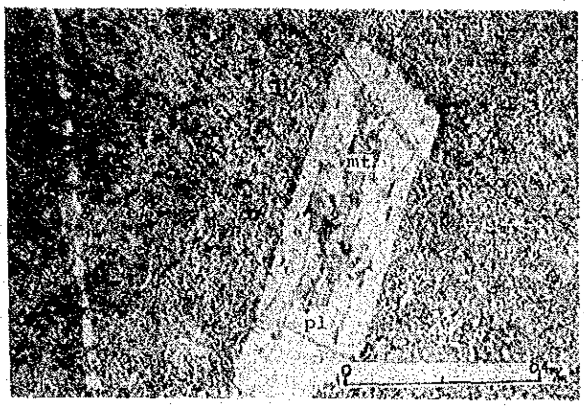

Fig. II–1–13b Microscopic Photograph of
Sample no. N–95,
augite andesite
porphyritic texture
groundmass ; cryptocrystalline

pl ; plagioclase
mt ; montmorillonite

(open nicol)

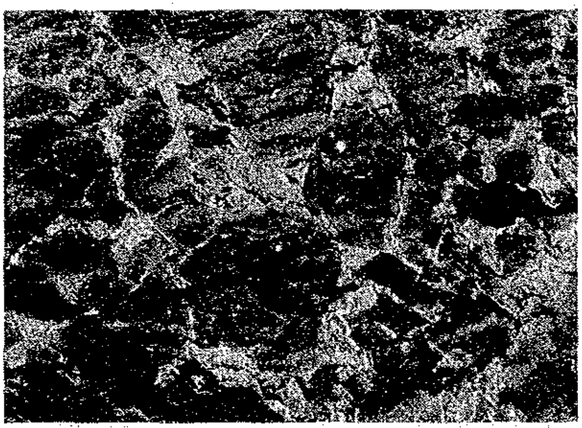

Fig. II–1–14a Photograph
(basaltic pillow lava, Batan river
pillow lava member, Buguias
formation at Agno river)
Sample no. N–96

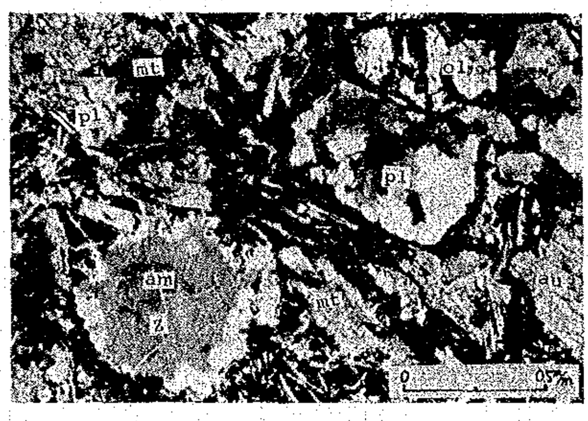

Fig. II–1–14b Microscopic Photograph of
Sample no. N–96
olivine augite basalt
amygdaloidal texture

pl ; plagioclase
ol ; olivine
au ; augite
mt ; montmorillonite
z ; zeolite
am ; amygdal

(cross nicol)

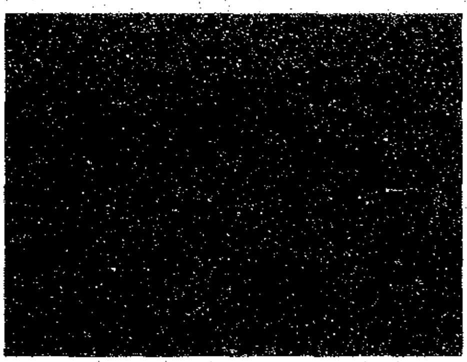

Fig. II–1–15 Photograph
(brecciated andesitic lava and pumice tuff, Nanayengan cr. andesitic volcanic member, Buguias formation at Route 11)

Fig. II–1–16a Photograph
(volcanic conglomerate of Loo formation at Dalimona)

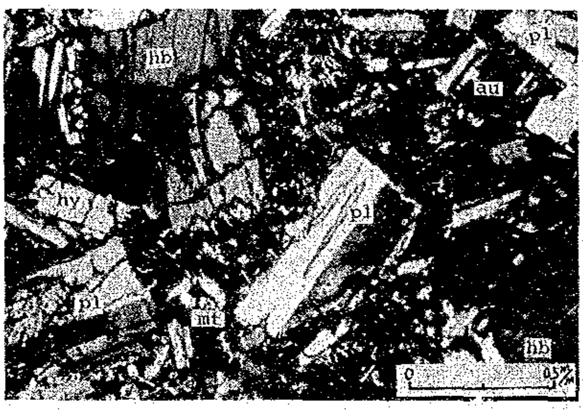

Fig. II–1–16b Microscopic Photograph of Sample no. M–46,
augite-hypersthene-hornblende andesite intersertal texture

pl ; plagioclase
hb ; green hornblende
hy ; hypersthene
au ; augite
mt ; montmorillonite

(cross nicol)

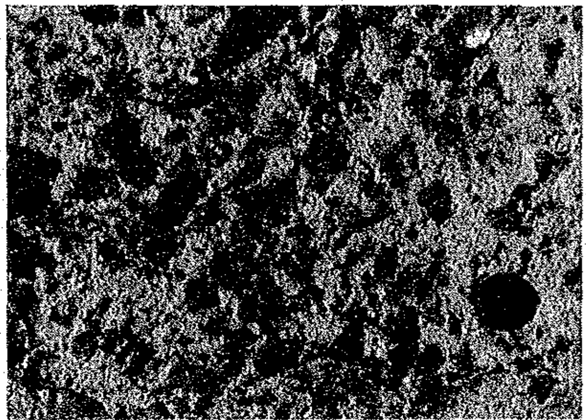

Fig. II–1–17 Photograph
(scoria and pumice bearing lapilli tuff, Loo formation at Loo)

conglomerates. The matrix of the rock contains abundant hornblende phenocrysts (Fig. II–1–16a). Pyroclastics show brown to bluish green color and contain volcanic breccia of hornblende andesite. The rock is generally porous. (Fig. II–1–17)

Compared with the Buguias formation, Loo formation is mainly composed of hornblende andesite and is poorly solidified as can be seen in the included breccia sticking out from the matrix. It is therefore, easily identified from Buguias formation.

Microscopic observation ; hypersthene augite hornblende andesite (Sample No. M–46) (Fig. II–1–16b)

Phenocryst ; plagioclase · hornblende · augite · hypersthene

Plagioclase phenocrystals are 0.6 ~ 2 mm long and they are shown a zonal structure and worm-eaten texture to be replaced by montmorillonite

1–4–3 Bodo Formation

Type locality : Bodo area at the north eastern part of Buguias. The formation is distributed at the eastern part of the survey area, partially covering lava domes and its surrounding area.

Thickness : 400 m±

Lithology : This formation is divided into two (2) groups, the lower and upper. The lower part of the formation is characterized by hornblende andesite, andesitic pyroclastic flow and volcanic mudflow intercalated with allophenized hornblende dacitic pumice fall (Fig. II–1–18). The upper part of the formation is mainly composed of dacite lava, which forms lava dome (Fig. II–1–20a) in the area, accompanied with biotite-hornblende dacitic pumice flow and lake deposits (Fig. II–1–19). Boundary of upper and lower groups is bordered by allophane soil, which shows a diastem of volcanic activities.

Dacitic volcanic mudflow of the lower group contains mainly hornblende dacite breccias and amygdaloidal basalt and altered rhyolite. The matrix consists of dacitic pumice. Carbonized wooden chips and altered rhyolite are observed in this mudflow.

Dacitic pumice flow of the upper group is porous and well graded, containing a significant amount of biotite, hornblende, and quartz grains.

The lava dome in this area is very similar to that of Daklan area both in lithology and in occurrence.

This formation is unconformably overlying the Loo formation.

Microscopic observation ; biotite hornblende dacite (Sample No. N–64) (Fig. II–1–20b)

Phenocryst ; plagioclase · quartz · hornblende · biotite

Plagioclase phenocrysts are predominant, 0.5 ~ 1.5 mm long, and They are composed of oligoclase to andesine shown zonal structures. Quartz phenocrysts are commonly 0.5 ~ 1.5 mm long and larger quartz ones are crashed.

Groundmass ; The groundmass is glassy and fresh. It is scattering quartz, plagioclase, biotite and hornblende.

1–5 Structural Geology

The geological structure of the survey area is characterized by intense faulting and block movement as observed at the center of Cordillera Central anticlinorium. The complicated geological structure in the area is represented by a combination of graben and horst with trends of N-S and E-W. The most predominant tectonic trend in the area is N-S, correlated to the Northern Luzon Arc direction, and subordinately E-W and NW-SE trends (Fig. II–1–21). Foldings and faultings took place from Miocene to Diluvial age and Quaternary volcanism occurred at the intersection of uplifted zones of N-S and E-W trends.

1–5–1 Folding Structure

Two types of folding structure with different scales showing N-S trend (specifically NNW-SSE) are developed in the area. The large scale folding extends several tens of Km along its axes with about 5 Km intervals. Small scale folding extends several Km along its axes with 10m to 1 Km intervals. These folding structures are unconformably overlain by Loo formation.

Large scale folding : Judging from the profile section, the folding is asymmetrical and shows box fold type with 0.8 Km intervals and wave crest line. This type of folding structure is continued from east to west in Mountain lake anticline, Buguias Central syncline, Pulibo Ridge anticline and Batan cyncline. All foldings are cut by fault systems in the area.

Among the folding structures, especially Buguias Central syncline which is piled up with thick sediments of Buguias formation is considered to have initiated the depression

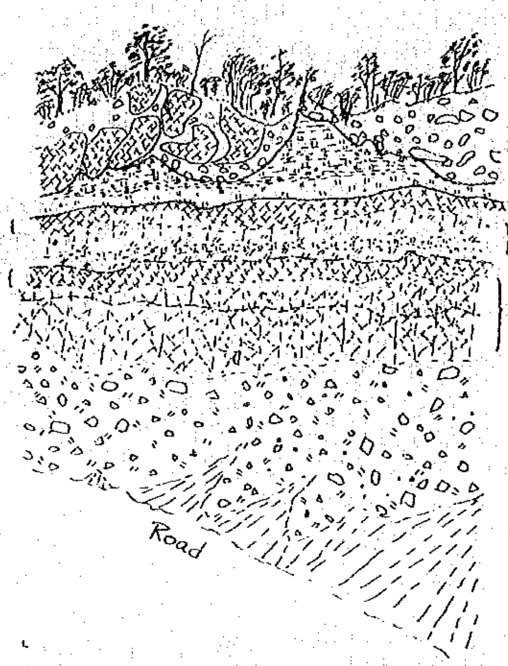

Fig. II–1–18 Sketch for a Outcrop of Bodo Formation

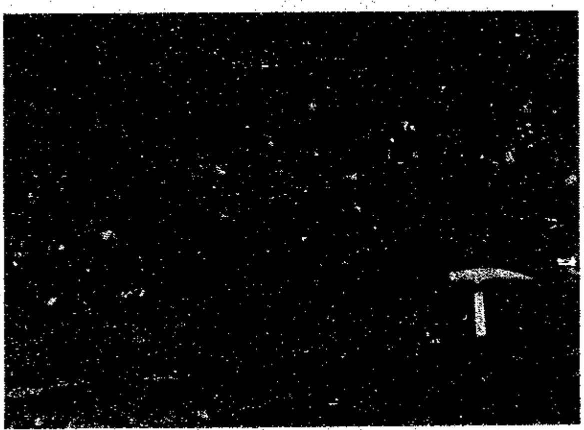

Fig. II–1–19 Photograph
(lake deposite, Bodo formation,
pumice representing a reverse grading,
beside of Mountain lake)

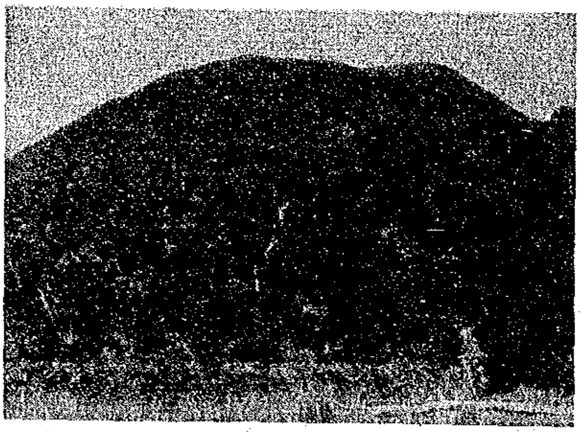

Fig. II–1–20a Photograph
(dacite lava dome of Budo formation, from Mountain lake)

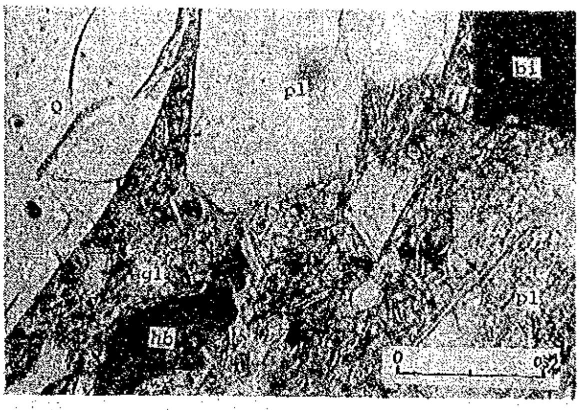

Fig. II–1–20b Microscopic Photograph of Sample no. N–112, augite bearing hornblende biotite dacite

pl ; plagioclase
Q ; quartz
bi ; biotite
hb ; hornblende

(open nicol)

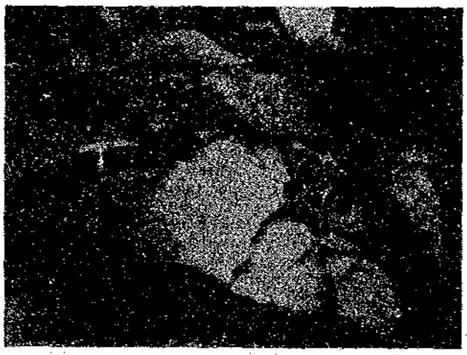

Fig. II–1–23a Photograph
(fine grain biotite-hornblende qtz diorite intruded in Buguias formation at Sinepsip)

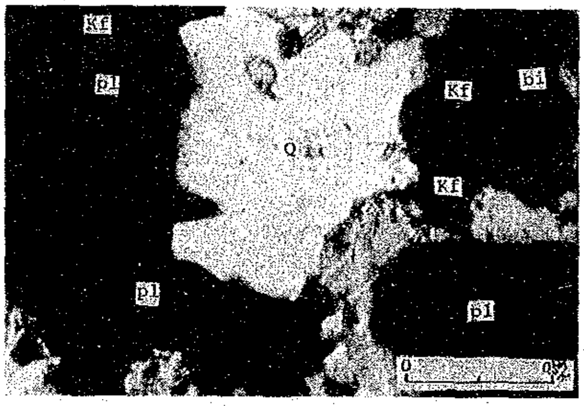

Fig. II–1–23b Microscopic Photograph of Sample no. M–67, biotite granodiorite

pl ; plagioclase
Q ; quartz
kg ; patassium feldspar
bi ; biotite

(cross nicol)

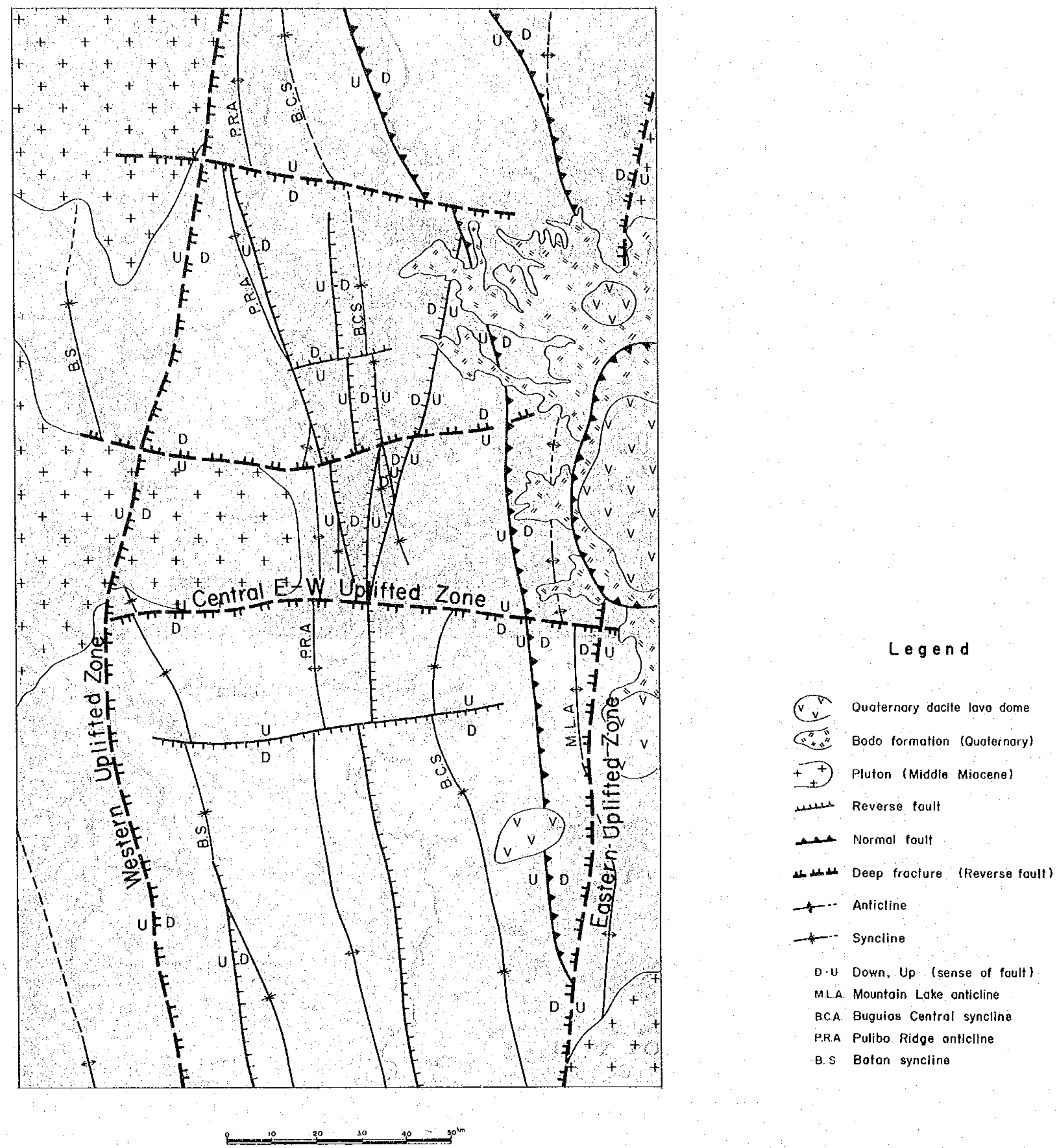

Fig. II–1–21 Tectonic Map

during the deposition of the formation.

Small scale folding : This folding structure is observed in Buguias creek alternating member and also in the sediments of Toking creek basaltic and andesitic member (Fig. II–1–22). The interlimb angles vary from gentle to steep. The fold of steep interlimb tends to develop at the Buguias Central syncline. Thus, small scale foldings are regarded as parasitic folds, which are minor folding in the incompetent sedimentary rocks, intercalated in major folded volcanic rocks. The folding mechanism is assumed as follows:

The thick sediments were deposited in Buguias Central syncline which was formed by a box folding in the sedimentation stage of Buguias creek alternating member. The box folding continued after the sedimentation and secondary lateral compression took place at the limbs of the syncline, forming the folds of steep interlimb in the incompetent sedimentary rocks. The box fold of large scale folding structure on the other hand, was formed in the competent volcanic rocks, which are composed of upper and lower parts of the sedimentary rocks.

1–5–2 Fault of Block Movement

As stated above, the most predominant fault system in the area is in a N-S trend, and subordinately E-W, NW-SE trends and ring form faults. High angle reverse faults and normal faults with block movement make the interpretation of the geological structures complicated. As shown by the distribution of plutonic rocks in the area, the block movements are characterized as uplifted zones in a N-S trend.

(1) N-S fault system

In general, N-S fault system consists of high angle reverse faults, traversing large scale fold and is cut by E-W and NW-SE trending fault systems. N-S fault system extends from Loo formation to Buguias formation, but does not affect to Bodo formation.

The faults are concentrated in the southern part of Buguias Central, corresponding to the form of Buguias Central synclinal structure. It may be suggested that a genetic relation between the formations of the synclinal structure and the N-S trend fault system exist. N-S trend faults found at the eastern and western parts of the survey area are elongated along the rimbs of uplifted plutonic rocks. The dislocation at the dip side is calculated to be 250m at the east of Buguias Central.

(2) E-W fault system

This fault system is represented by high angle reverse fault, which is located at the E-W trends uplifted zone.

(3) NW-SE fault system

This fault system is mainly observed at the eastern part of the survey area with the normal fault dipping to the east. The fault displaces Loo formation showing a crisscross relationship with the E-W system.

The apparent thickness of Loo formation is magnified by the dislocation caused by this fault system.

(4) Ring form fault system

Ring form depression is observed around Mountain Lake, surrounding Mt. Lusab, one of the Quaternary dacite lava domes. At the topographically low place caused by ring form fault, aqueous sediment of pumice is observed. This fault is considered to have collapsed into a circular form during the time of eruption and the uplift movement of the lava dome.

1–5–3 General Feature of Geological Structure

According to the geological reports, Geology of Daklan Area (B.E.D., 1980) and the Collaborated Mineral Exploration (MMAJ, 1977), the basement in the area is considered to be Kpg, basic volcanics of Palaeocene to Eocene, which are eugeosynclinal sediments. The basement in the area is presumed to be affected by the Sierra Madre orogeny. This orogeny was a tectonic movement that segregated the anticlinorium and synclinorium areas with a N-S trend at Paleogene to Neogene.

Cordillera Central, area of anticlinorium, was a locality of erosion in Oligocene. However, the raptures of N-S trend took place in the whole survey area in late Oligocene. During Miocene, the area subsided to a shallow water environment by transgression. Thus, basaltic lava was erupted and formed thick pillow lava formation. Thereafter basaltic and andesitic eruption followed, forming hyaloclastites, pyroclastics members with calcareous materials containing marine fossils. These volcanic activities progressed in a shallow water environment accompanied with rhyolite lava locally. Therefore, polymodal volcanics is prevalent in this stage.

Succeeding polymodal volcanic activity and sedimentation followed. The sedimentation proceeded to pile up the submergence of the sedimentary basin, which was caused by the N-S block movement.

Conglomerates derived from basement rocks in Buguias formation were transported from the south, the upheaved area during the deposition of the formation.

Andesitic pyroclastics, basaltic pillow lava, hyaloclastite and andesitic pyroclastics followed and thus Buguias formation was formed in the early stage of Miocene.

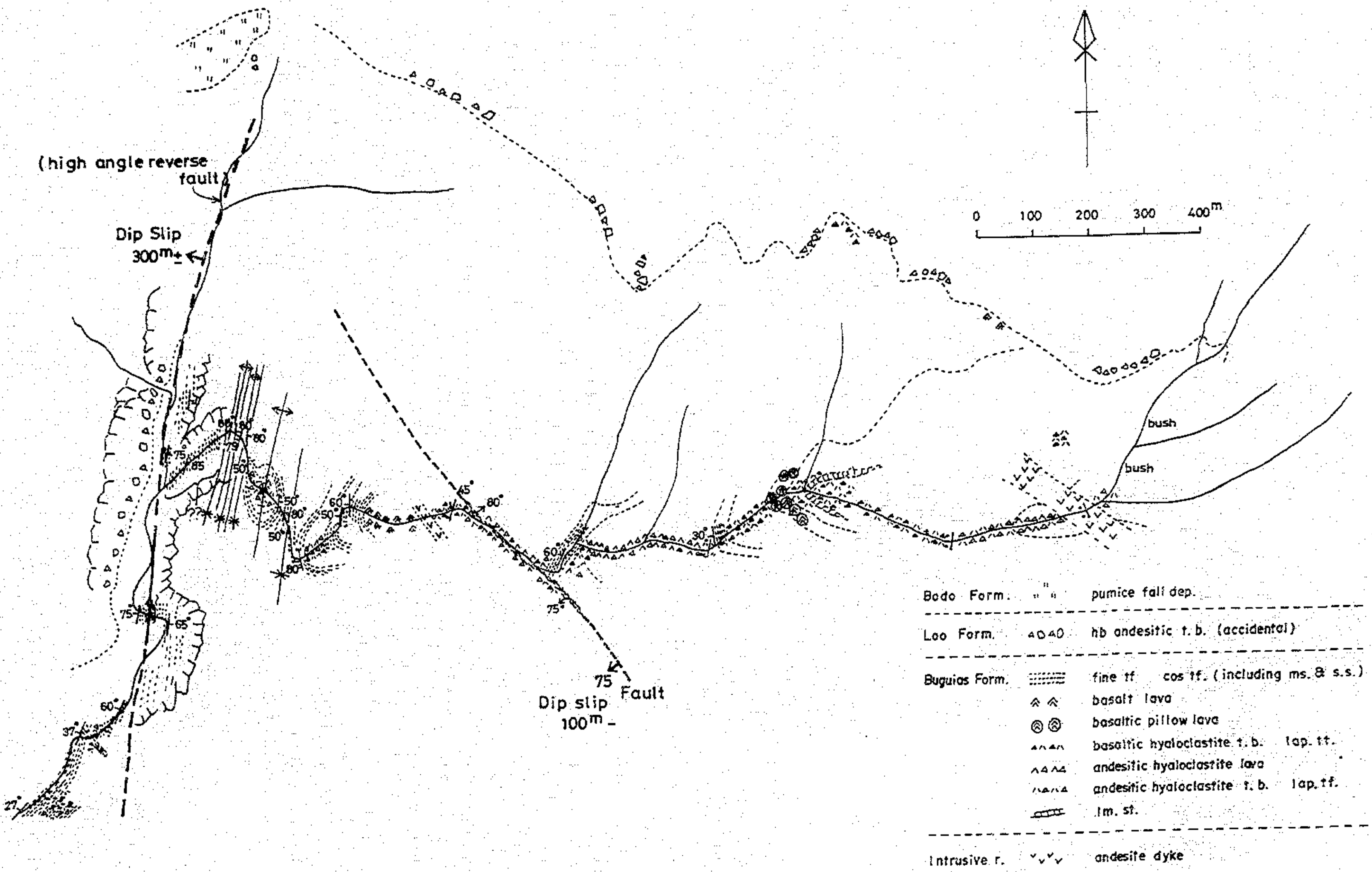

Fig. II−1−22 Minor Folds of the Northern Branch of Buguias Cr.

After the deposition of Buguias formation, quartz diorite and granodiorite, which were emplaced at the eastern and western parts of the survey area intruded into the Buguias formation in a N-S trend. Thereafter, the area was uplifted. The process of the plutonic activity and block movement trending E-W was then initiated.

In late Miocene, terrestrial sediments derived from andesitic and dacitic activities were formed at the northeastern and south-western parts of the survey area.

In Quaternary, dacite lava domes were formed at the intersection of E-W and N-S uplifted zones at a N-S trend at the eastern part of the survey area.

1–6 Igneous Activity

In the surveyed area Tertiary and Quaternary formations are mainly composed of volcanic rocks and intruded by a large number of igneous rocks.

The lowest member of Buguias formation, Kayapas creek pillow lava member mainly consist of basaltic pillow lava of augite olivine basalt. Toking creek basaltic and andesitic volcanics member conformably overlies Kayapas creek pillow lava member and is mainly composed of pyroclastic rocks and lava which often formed pillow lava and hyaloclastite. The volcanic rocks are augite andesite to augite basalt. This member is locally accompanied by rhyolitic lava indicative of culmination of bimodal volcanic activity.

Buguias creek alternating member was deposited when volcanic activity ceased. After a long volcanic dormancy, augite andesite was erupted, followed by the extrusion of olivine basaltic pillow lava, pyroxene andesite and altered NW-SW trending pyroxene andesite dike which intrudes into a part of Buguias formation. The dike was considered to be of the same age as the Buguias formation.

In middle Miocene, intrusion of hornblende-biotite quartz diorite (Fig. II–1–23a, II–1–23b)accompanied with biotite granodiorite followed with a N-S trend and were observed to crop out in the eastern and western edge of the surveyed area. In addition, they overhang eastward in Natubleng. The intrusion of this pluton formed the base of a trellised block structure trending N-S and E-W.

In late Miocene the continental volcanic eruptive activity controlled by the trellised block structure had taken place in the northeastern and southwestern part of the area, and the rocks are characterized by augite hypersthene hornblende andesite (Fig. II–1–24a, Fig. II–1–24b) and augite hypersthene hornblende dacite. In the Loo formation the intrusion of the same granitic rocks showing the same N-S and E-W trends occurred simultaneously with the above eruptive activity.

In uppermost Miocene the activity of a complex N-S and E-W trending complex (Fig. II–1–25a, Fig. II–1–25b) of quartz diorite porphyry, diorite porphyry and dacitic porphyry took place.

Furthermore, in late Pleistocene the acidic volcanic rocks was extruded around the intersection of eastern N-S uplifted zone and central E-W uplifted zone. The volcanic activity is the pyroclastic flow of biotite-hornblende andesite with abundant breccia followed by the pumice fall deposit of biotite-hornblende dacite, then the pumice fall deposit and lava dome eruption (inferred minimum capacity : 7 Km^3) of augite-biotite andesite. It is inferred that the activity was changing to more silicic composition with respect to time.

1–7 Geothermal Alteration

The alteration in the surveyed area is classified into three types, namely regional burial metamorphism, mineral alteration, and geothermal alteration. Regional burial metamorphism is observed in the whole of Buguias formation and part of Loo formation as the green coloured argillization (Fig. II–1–26, II–1–27). Mineral alteration consists of pyritization and silicification related to plutonic rocks in the northwest of the area, volcanic to plutonic rocks in the central part and rhyolite porphyry (Fig. II–1–28). Geothermal alteration of the area is isolated in distribution.

The green coloured argillization of regional burial metamorphism could be differentiated from that of geothermal alteration by the following: The former generally spread widely and is homogeneous, whereas the latter is mostly heterogeneous and restricted in distribution.

1–7–1 Alteration Zone

In the surveyed area, the geothermal alteration zone is only distributed along the upstream of Toking creek, 100m long. Around the area the unreported geothermal alteration zone was found along the stream, about 4 km east of Batowan pass.

Geothermal alteration zone along the upstream of Toking creek

The zone extends in the direction of N-S and is characterized by white coloured argillization and silicification. The alteration varies from higher grade where rocks were completely altered and their texture vague, to lower grade where rocks were altered only partially. The original rock is rhyolite dike. The dimension of this zone is not clear because the survey was conducted along the creek only.

The X-ray diffractive analysis (Fig. II–1–29 a, b, c) reveals that alunite, α

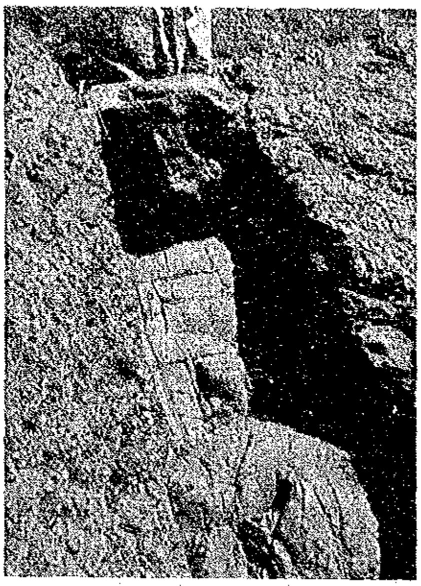

Fig. II–1–24a Photograph
(hornblende andesite dyke intruded in Loo formation in Kayapas creed)
Sample no. M–37

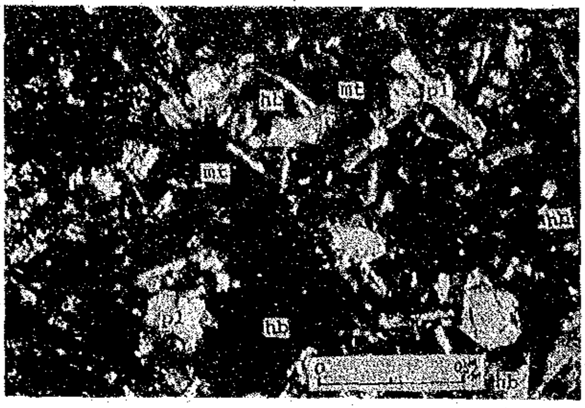

Fig. II–1–24b Microscopic Photograph of Sample no. M–37, hornblend andesite porphyry

pl ; plagioclase
hb ; hornblende
mt ; montmorillonite

(cross nicol)

Fig. II–1–25a Photograph
(rhyorite dyke with platy joint, intruding in Loo formation in Toking creek)
Sample no. N–71

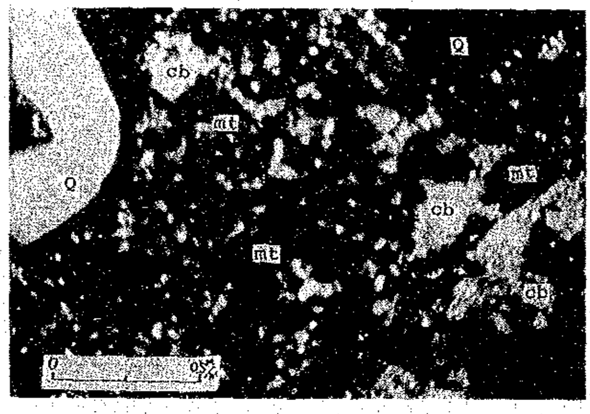

Fig. II–1–25b Microscopic Photograph of Sample no. N–71

Q ; quartz
cb ; carbonate mineral
mt ; montmorillonite

(cross nicol)

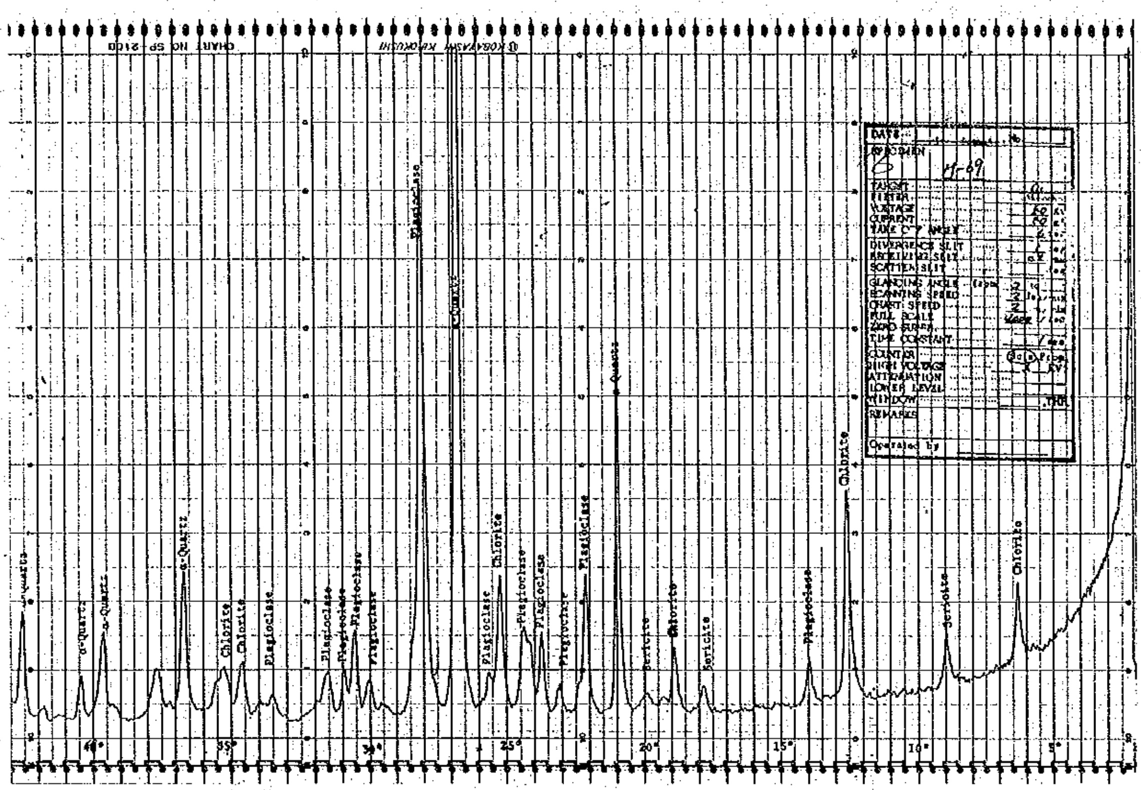

Fig. II–1–26 X-ray Diffraction Chart of Sample No. M–69

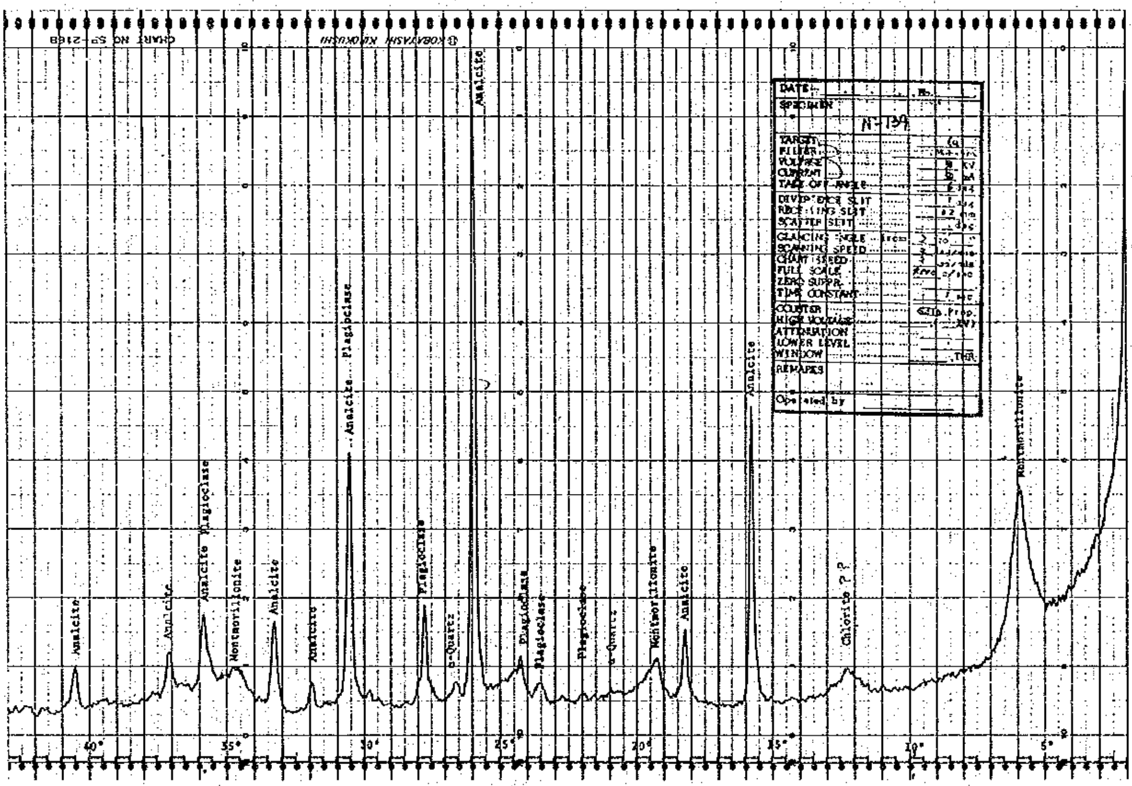

Fig. II–1–27 X-ray Diffraction Chart of Sample No. N–139

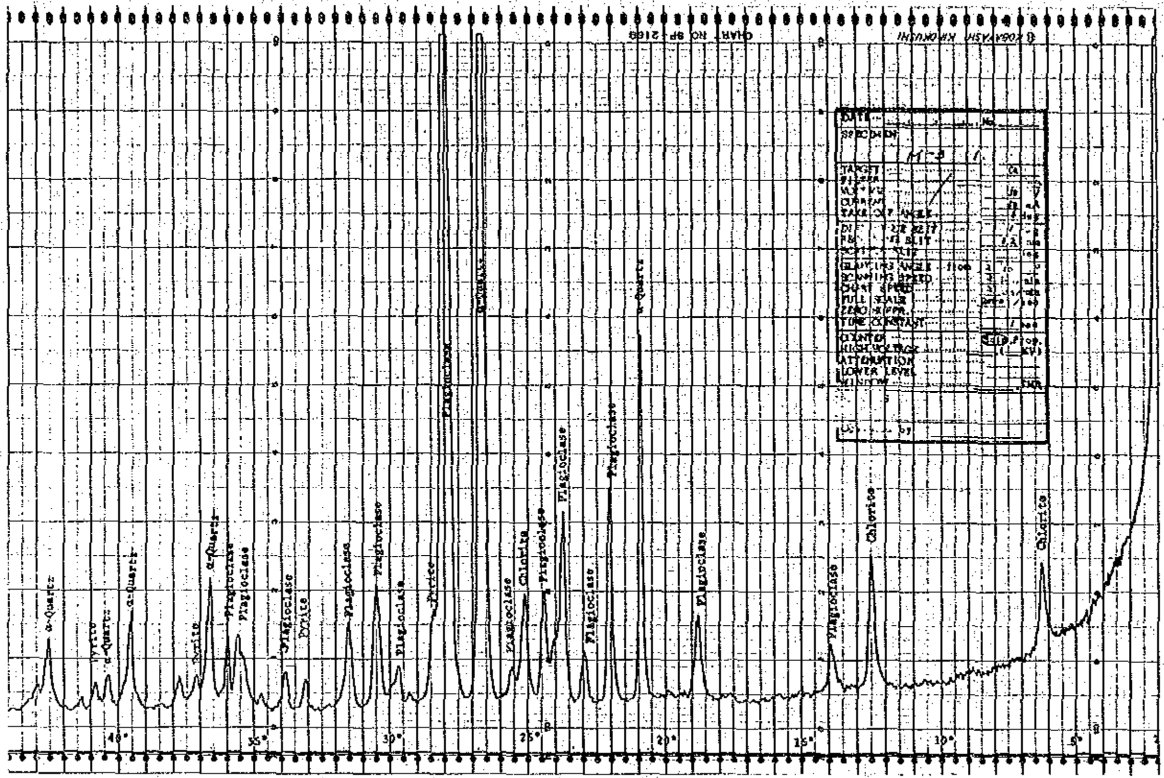

Fig. II–1–28　　X-ray Diffraction Chart of Sample No. M–3

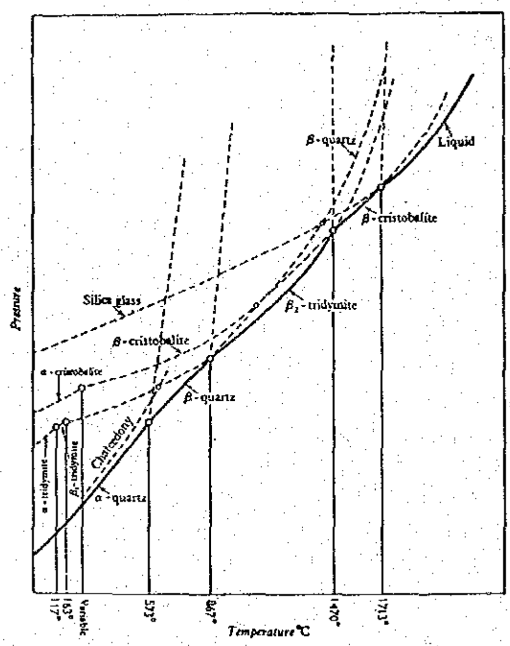

Fig. II–1–31　　The Stability Relation of the Silica Minerals after Fenner (1913)·

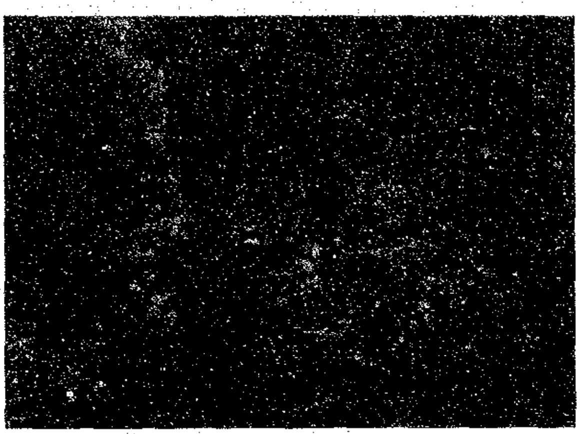

Fig. II–1–29a Photograph
(alunite alteration zone in
Toking creek)
Sample no. N–63

Fig. II–1–29b Microscopic Photograph of
Sample no. N–63

si ; silica mineral
al ; alunite

(cross nicol)

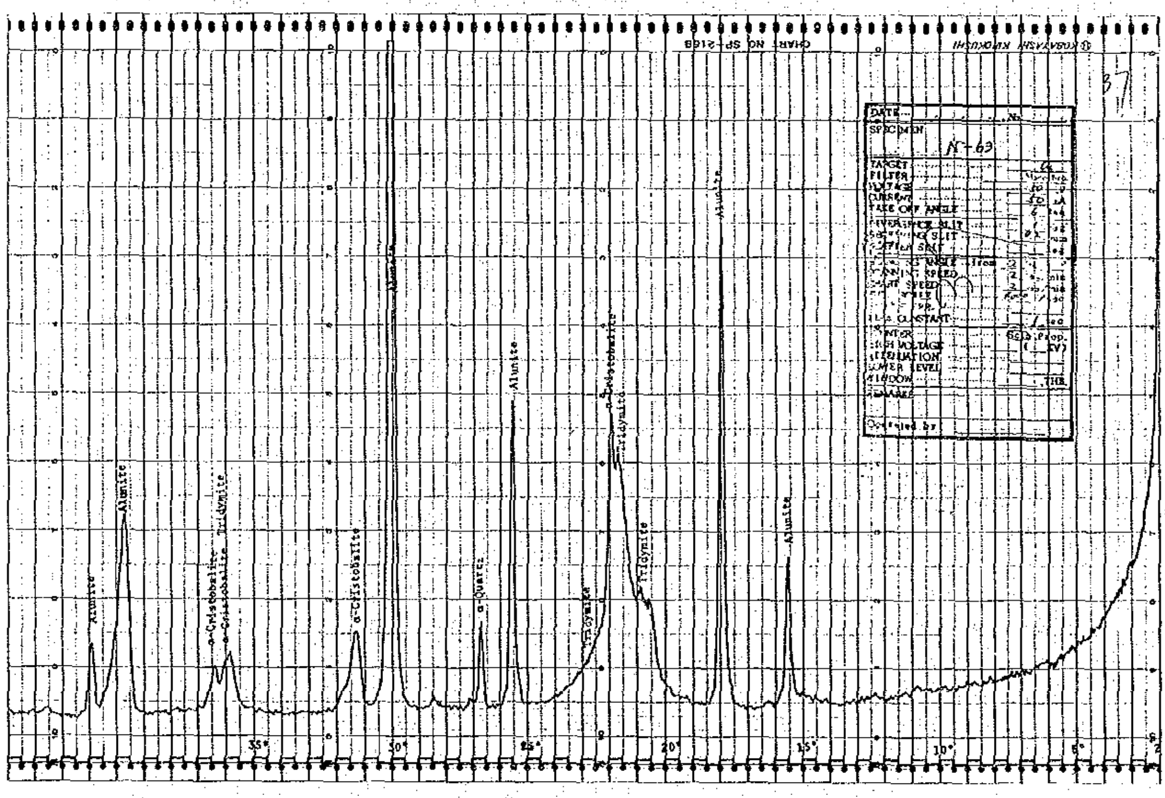

Fig. II–1–29c X-ray Diffraction Chart of Sample No. N–63

-cristobalite and tridymite are abundantly produced as secondary minerals in the portions of strong argillization and silicification. It shows the combinating of alunite and silicate minerals.

At present no hot spring is observed along the creek. The quaternary mud-flow around 1500m in elevation crops out along the slope of the right bank at the mouth of Toking creek and it contains a large amount of gravels showing similar rock facies to the geothermal alteration zone. The matrix of the mud-flow is composed of white clay with imperfect carbonized wooden pieces and lithic fragments of altered rhyolitic rocks and rocks of Bugias formation. The breccia is of altered rocks mentioned above and of rocks of Buguias formation, unaltered by geothermal fluid.

The X-ray diffractive analysis reveals that this breccia of altered rocks contains alunite, kaolinite and silicate minerals as altered minerals. This combination of minerals suggests that the alteration had been carried out in an acidic condition and below 100°C. Therefore the breccia could be the product of a fumarolic activity. These facts support the idea that the mud-flow was transported from a geothermal alteration zone. It formed after the deposition of Bodo formation suggested by an embedded imperfectly carbonized wooden piece and it is an alluvial deposit. In Bodo formation there is no evidence of mud flow unit ascribed to geothermal alteration.

Geothermal alteration zone, 4 Km east of Bodoan pass

The alteration zone is observed in Bodo formation and shows white silicification and argillization (Fig. II–1–30a). The zone extends more than 200 m x 50m. However, data of accurate dimension and the trend was not obtained, so it is necessary to do more investigation.

This alteration zone is accompanied with boiling hot spring and fumarolic activity and is situated in the transitional place of the topography changing from steep to gentle slope eastward from Mt. Lusab. The altered zone is in the dacitic, pyroclastic flow of Bodo formation, and native sulfur is produced near the fumarole (Sample No. P-1 Fig. II–1–30b, II–1–30c).

The X-ray diffractive analysis reveals that the secondary minerals of white coloured silicified portion (Sample No. P-1) consist of α-quartz, tridymite and α-cristobalite. The peaks of α-cristobalite are very sharp on the X-ray chart and it suggests that the crystallinity is high.

Kinbara (1977) considered that the inverstion of α-cristobalite to α-quartz takes place approximately below 100°C. This tridymite shows similar pattern of peaks to the low-temperature tridymite on ASTM cards which are 1–0378 and 3–0227. The peaks of α-quartz are not sharp and it indicates that the crystallinity is low.

This mineral assemblage, α-quartz tridymite, α-cristobalite supports the idea that the alteration has taken place at 100°C ± (Fig. II–1–31).

Fig. II–1–30a Photograph of fume alteration zone with hot springs of 96°C in Ifugao side Sample no. P–1

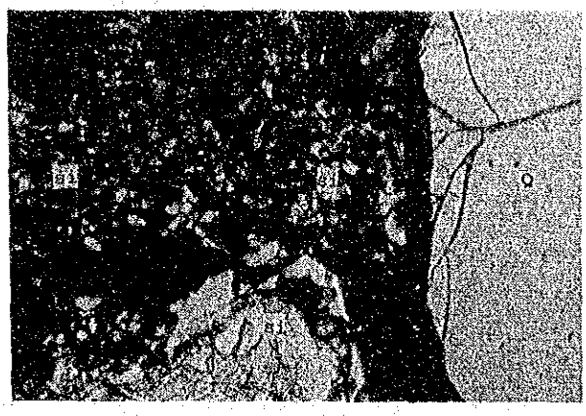

Fig. II–1–30b Microscopic Photograph of Sample no. P–1, altered dacite of Bodo formation

Q ; quartz
si ; silica mineral replacing all minerals except quartz.

(open nicol)

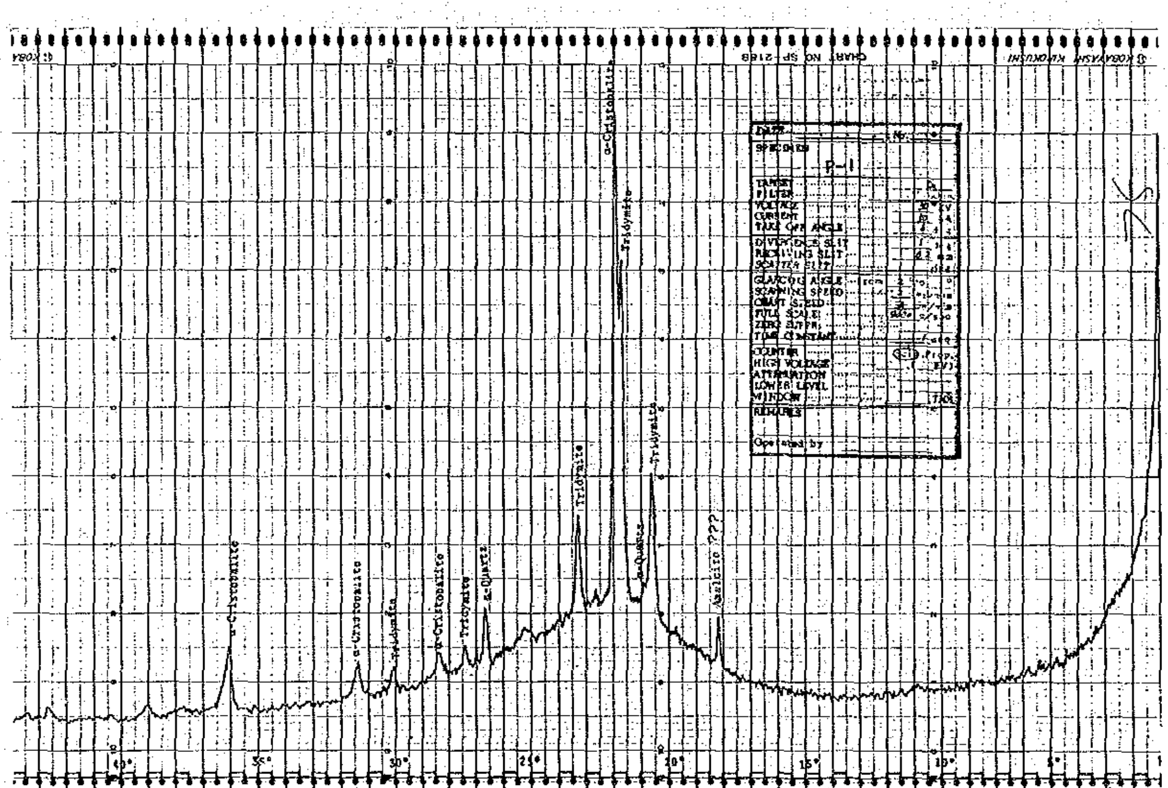

Fig. II–1–30c X-ray Diffraction Chart of Sample No. P–1

CHAPTER 2

GEOCHEMICAL EXPLORATION

Chapter 2
Geochemical Exploration

2–1 Purpose and Method of the Survey

Geothermal manifestation as represented by geysers, fumaroles, and hot water springs as geothermal indication on the surface is considered to be derived from geothermal energy existing in the aquifer under subsurface conditions.

Objectives of this geochemical exploration are to study the geothermal indications on the surface of the Buguias geothermal field, to deduce the temperature of the subsurface geothermal reservoir from the chemical compositions of the geothermal field, and to find out the probable location of the heat source from the distribution of the sinter deposits derived from hot springs prevailing in the area and also from the distribution of geothermal alteration zones as a consequence of hot water underground circulation.

One meter depth hole for temperature measurement

In order to determine the temperature gradient on the surface, eighty three (83) holes of one meter depth were made and the bottom temperature was measured in the Buguias Central area, wherein hot water springs are located.

The survey lines at 200m to 400m intervals were laid trending on a N-S direction on each site of the road, apparently crossing a supposed subsurface flow of geothermal water.

The one meter holes were drilled at 50m intervals avoiding rice fields and topographical effect. For this reason the survey lines and stations were not established in a straight course and definite interval. All the holes were surveyed and mapped using Brunton compass. (Fig. II–2–1, II–2–2).

The holes were drilled by a hand auger, and immediately after the completion of each hole the bottom hole temperature was measured with a thermistor, A–600 Model of Takara.

Geochemistry of the hot springs

At the time of hot water sampling, temperature and pH values of hot water were measured at the site. Nine (9) hot water samples and one (1) creek water sample were taken in 3,000 ml polyethylene vessels for chemical analysis. Hydrochloric acid was added to each water sample to have a pH = 2.0. These water samples were brought to Japan and analyzed for seventeen (17) principal elements, pH, electrical conductivity, TSM, Li^+, B^+, Na^+, K^+,

Ca^{+}, Mg^{+2}, total Fe, Al^{+3}, F^{-}, HCO_3^{-}, SO_4^{-2}, As, SiO_2, and SiO_2^{x}, at the Bishimetal Exploration Co. Chemical Laboratory. Equipment used and method of analysis are as follows.

pH	:	Basing on JIS Z8802, F-7 type pH meter used.
Electric conductivity	:	CM-2A type, Towa-Dempa Co. used.
Li^{+}	:	Flame spectrochemical analysis employed.
B^{+}	:	Colorimetric analysis employed.
Na^{+}	:	Used Hitachi-518 atomic absorption spectrometer
K^{+}	:	Used Hitachi-518 atomic absorption spectrometer
Ca^{++}	:	EDTA titration.
Mg^{++}	:	EDTA titration.
Total Fe	:	Used 6B type spectrometer.
Al^{+++}	:	Used 6B type spectrometer.
F^{-}	:	Used 6B type spectrometer.
HCO_3^{-}	:	Titrated with 1/20N HCl standard solution.
Cl^{-}	:	Titrated with mercury nitrate standard solution.
SO_4^{--}	:	Measured barium sulfate with direct reading balance.
As	:	Used 6B type spectrometer.
SiO_2	:	Measured with direct reading balance. (gravimetric analysis)
SiO_2	:	Total silica was measured by colorimetric analysis.
Temp (°C)	:	Used A-6000 Model, Takara.

2–2 Temperature Measurement of One Meter Hole

The bottom temperature of a shallow hole, in general, would be affected by surface conditions, such as altitude of location, atmospheric temperature, sunshine hours, infiltration of ground water and other surface factors. In order to insure the uniformity of measurement conditions, the locations of eighty three (83) holes were selected at the following places (Table II–2–1).

1) Plain field and slope facing south-west were chosen to receive equal sunshine hours.
2) Avoiding forest and shade of houses, grass field was selected.
3) Avoiding ill effect from infiltration of ground water, site was selected at the hillside of irrigation channel.
4) Field sprinkled with water was avoided.

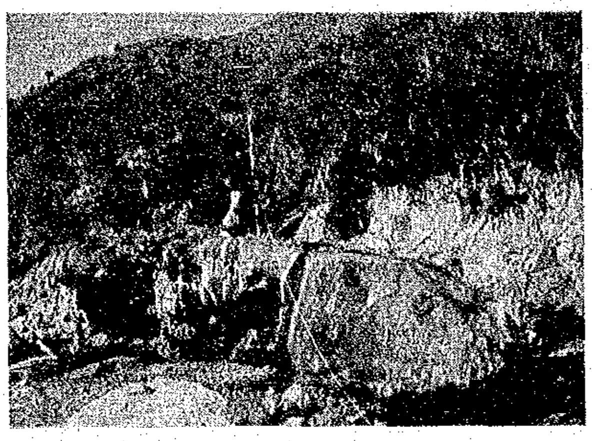

Fig. II–2–1 Photograph

(Geochemical Survey of Traverse Survey)

Fig. II–2–2 Photograph

(Geothermal Survey of 1 m Depth)

Table II–2–1 One Meter Gradient Holes

	Temp.	Time	Date	Location/Remarks
1.	21.5	2:26	3–2–81	Starting point. Uphill north from camp. Located near a big pine tree.
2	22.0	2:32	3–2–81	Around 25 meters WWS from Bug - 1.
3	18.5	2:41	3–2–81	Shallow hole, loose stony formation down east of No. 1 along a dried creek shaded with shrub vegetations.
4	17.5	2:45	3–2–81	Shaded with grasse and a small tree. Located a few meters uphill SSE of No. 3.
5	21.0	2:50	3–2–81	A few meters down west from the road after the creek going to camp partly shaded by banana plants.
6	21.5	2:54	3–2–81	Near mud pool covered with weeds.
7	20.5	3:00	3–2–81	Wet bottom hole of probably the same geology as of No. 6.
8	20.5	3:04	3–2–81	A few meters uphill east from the road near the blind curve.
9	20.0	3:08	3–2–81	50 meters south of No. 8.
10	20.5	3:10	3–2–81	
11	23.0	3:32	3–2–81	
12	20.0	1:45	2–28–81	A few meters from camp slong the road.
13	23.2	8:20	3–2–81	Reference Point gradient hole. Located a few meters down the south wing of the Barrangay Captain Iguado's residence.
14	21.0	2:05	2–26–81	A few meters up the road near the north boundary of the school.
15	19.0	2:25	2–26–81	A few meters away from a thermal manifestation.
16	25.0	2:35	2–26–81	Opposite bank of Bug-1 near the Man-Atong Bridge shaded partly by banana plants.
17	21.0	3:10	2–26–81	Located uphill at the back of the school.
18	20.0	3:20	2–26–81	Uphill 50 meters away from No. 17 going south.
19	25.0	8:50	2–27–81	Further south of No. 18. Hole covered with soil after a day visibly by termite activity.
20	22.0	8:53	2–27–81	Down hill south of No. 19.
22	28.0	9:27	2–27–81	A few meters uphill of Bug-10.
23	31.0	9:40	2–27–81	A few meters after the Asinan-Sedel Bridge south and located near the road.
24	27.0	9:50	2–27–81	Located further south of No. 23 not far from the road.
25	32.0	10:05	2–27–81	Along the road, a few meters west of warm spring (Bug. 12) which was sampled.
26	24.0	10:10	2–27–81	
27	19.0	10:30	2–27–81	
28	18.0	10:35	2–27–81	
29	19.0	10:55	2–27–81	
30	23.0	11:10	2–17–81	
31	18.0	11:15	2–17–81	Slightly wet bottom hole.
32	19.0	11:25	2–27–81	
33	19.5	11:30	2–17–81	
34	21.0	11:45	2–17–81	Located along the road overlooking Buguias Creek
35	22.0	1:45	2–27–81	
36	23.0	2:00	2–27–81	
37	23.5	2:05	2–27–81	
38	24.0	2:20	2–27–81	
39	50.0	2:24	2–27–81	
40	24.0	2:50	2–27–81	
41	20.5	3:05	2–27–81	
42	18.0	2:42	2–27–81	Colder temperature may be due to the effect of irrigation water.
43	27.0	3:28	2–27–81	
44	22.5	3:35	2–27–81	
45	20.0	3:45	2–27–81	
46	20.0	3:57	2–27–81	
47	21.5	4:05	2–27–81	
48	21.5	4:15	2–27–81	The hole is drilled near the house. The bottom hole is slightly moist.
49	21.5	8:45	2–28–81	
50	22.0	8:48	2–28–81	
51	18.5	8:57	2–28–81	Shaded cite.
52	17.5	9:37	2–28–81	Shaded cite.
53	21.5	10:16	2–28–81	
54	21.5	10:19	2–28–81	
55	22.5	10:23	2–28–81	
56	24.0	10:38	2–28–81	
57	22.0	10:55	2–28–81	
58	18.5	10:52	2–28–81	
59	21.5	11:50	2–28–81	
60	19.5	1:46	2–28–81	
61	20.0	2:09	2–28–81	
62	23.5	2:18	2–28–81	
63	18.5	2:24	2–28–81	
64	23.5	2:31	2–28–81	
65	21.0	2:45	2–28–81	
66	21.0	2:41	2–28–81	
67	22.0	3:17	2–28–81	
68	22.5	3:25	2–28–81	
69	18.0	3:44	2–28–81	
70	20.0	3:40	2–28–81	
71	21.5	3:52	2–28–81	
72	21.0	4:02	2–28–81	
73	22.0	9:38	2–28–81	
74	22.0	10:36	3–1–81	Shallow hole (hard soil formation)
75	18.0	11:00	3–1–81	
76	17.0	11:05	3–1–81	
77	18.0	11:09	3–1–81	
78	20.0	11:30	3–1–81	
79	19.5	11:37	3–1–81	
80	21.0	12:08	3–1–81	
81	17.0	12:15	3–1–81	
82	20.5	12:30	3–1–81	
83	17.5	12:36	3–1–81	

In case of low latitude and high altitude places like the Buguias area, it was considered that bottom hole temperature of one meter depth might be affected by atmospheric temperature. Hole No. 13 was therefore chosen as a reference standard hole. Almost hourly variation of bottom hole and atmospheric temperature were observed for several days as shown in Fig. II–2–3. Observation of the standard hole revealed that the bottom temperature did not encounter any significant change and was therefore valued at 23.2°C with no correction made. Likewise, it was deemed not necessary to make any altitude corrections for the change would be minimal. Altitude correction in Japan where the holes are sited at over 1,000m above sea level would be 0.4 – 0.5°C per 100m change of elevation.

The value of the bottom hole temperature obtained showed a normal distribution (Fig. II–2–4). Six (6) holes are over 27.0°C and are considered significantly anomalous. The average temperature including the anomalies came up to 21.3°C, while excluding the anomalies the value is 20.8°C and its standard deviation is 2.0 (Fig. II–2–5).

A series of isothermal lines were mapped as a result of the survey. There were five (5) distinct temperature groupings made. The map gives the following information:

1) The high temperature zones appear at or around geothermal manifestations as a whole, and low temperature zones are situated in the north, the south and on the east of the surveyed area, indicating that these zones are far from the heat source.

2) Four (4) distinct high temperature zones were observed trending east to west, inferring the same direction of the hot water flow.

3) Each high temperature zone, however, occurs from the east of the Agno river up to the road. The eastern end of the zones is noted to be parallel to the level contour line of 1,400m A.S.L.

The facts mentioned above give us the following ideas on the geothermal system in the area.

1) The high temperature zones extending east to west indicate flow direction of hot water near the surface.

2) The low temperature zones which appeared at the north, south and east of the area are considered to be normal surface temperatures in the area and suggest that these areas are far from the heat source.

3) The low temperature zones at the north and the south therefore showed that the hot water flow did not exist near the surface or is situated at a deeper place in the area.

4) The fact that the eastern end of the high anomalous zone coincides with the 1,400m

contour line of elevation, is indicative of the water table in the area. This suggests that the water table possibly becomes deeper toward the eastern side, as an effect of changes in topographical conditions.

Considering the facts mentioned above, it is recommended to drill deeper in order to penetrate the aquifer, whenever the drill site is established above 1,400m. On the other hand, the geothermal fluid would flow out from the wellhead during drilling operation even on shallow depths, in case the drilling site is located below 1,400m A.S.L.

2–3 Geochemistry of Hot Springs

Almost all of the existing geothermal manifestations located in the area were roughly surveyed and their localities were connected with a base point (BM–1) and mapped. As shown in Fig. II–2–5, all manifestations are distributed at the east and west bank of the Agno river around the area of Buguias Central.

The geothermal manifestations in the area are characterized by hot water flow and gas bubbling pools at some areas. Sinter deposits which are mainly composed of calcium carbonate are distributed around the whole area of manifestation. The general features of hot spring activity is shown in Table II–2–2. Of these samples, eight (8) warm springs (No. 1, 3, 4, 5, 6, 9, 10 and 13) were taken and four (4) of them (No. 1, 5, 7 and 10) were also selected for gas sampling. One (1) creek sample No. 15 and one (1) cold ground water were taken at eastward of Buguias Central.

The temperature and pH value of hot water were measured during the sampling at the site by an alcohol thermometer, a thermistor A-600 Model and pH meter HM-1K Model. Samples taken were accommodated in 3,000 ml polyethylene vessels and some of them were modulated to pH = 2 by addition of HCl. These samples were brought to Japan for chemical analysis. Gas samples were taken in gas collectors and sent to B.E.D. laboratory for gas analysis.

The temperature of hot water which flows out from cracks of rocks and travertine ranges from 40°C to 71°C. The field pH values are from 6.1 to 8.1 measured with a pH portable meter. Some of the hot springs (No. 1, 2, 5, 7, 9 and 10) are associated with moderate gas bubblings.

The gas is mostly carbon dioxide (CO_2) with almost nil amount of hydrogen sulphide (H_2S). Using Kitagawa type tube method of field analysis, 1.5 ppm H_2S was recorded and carbon dioxide was over 97% of the total gas content, considering from absorption rate into

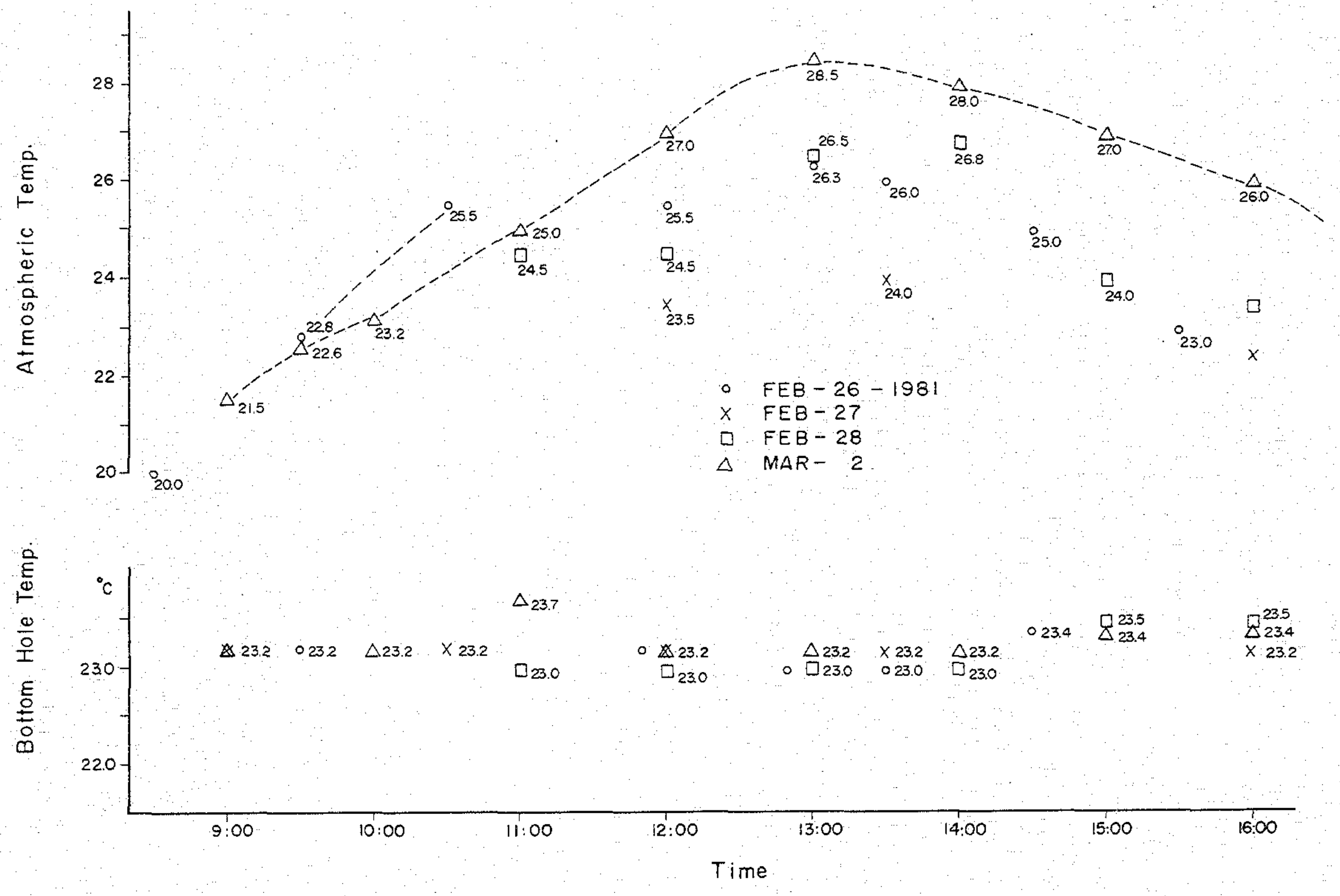

Fig. II–2–3 Daily Variation for Geothermometry of 1 m Depth

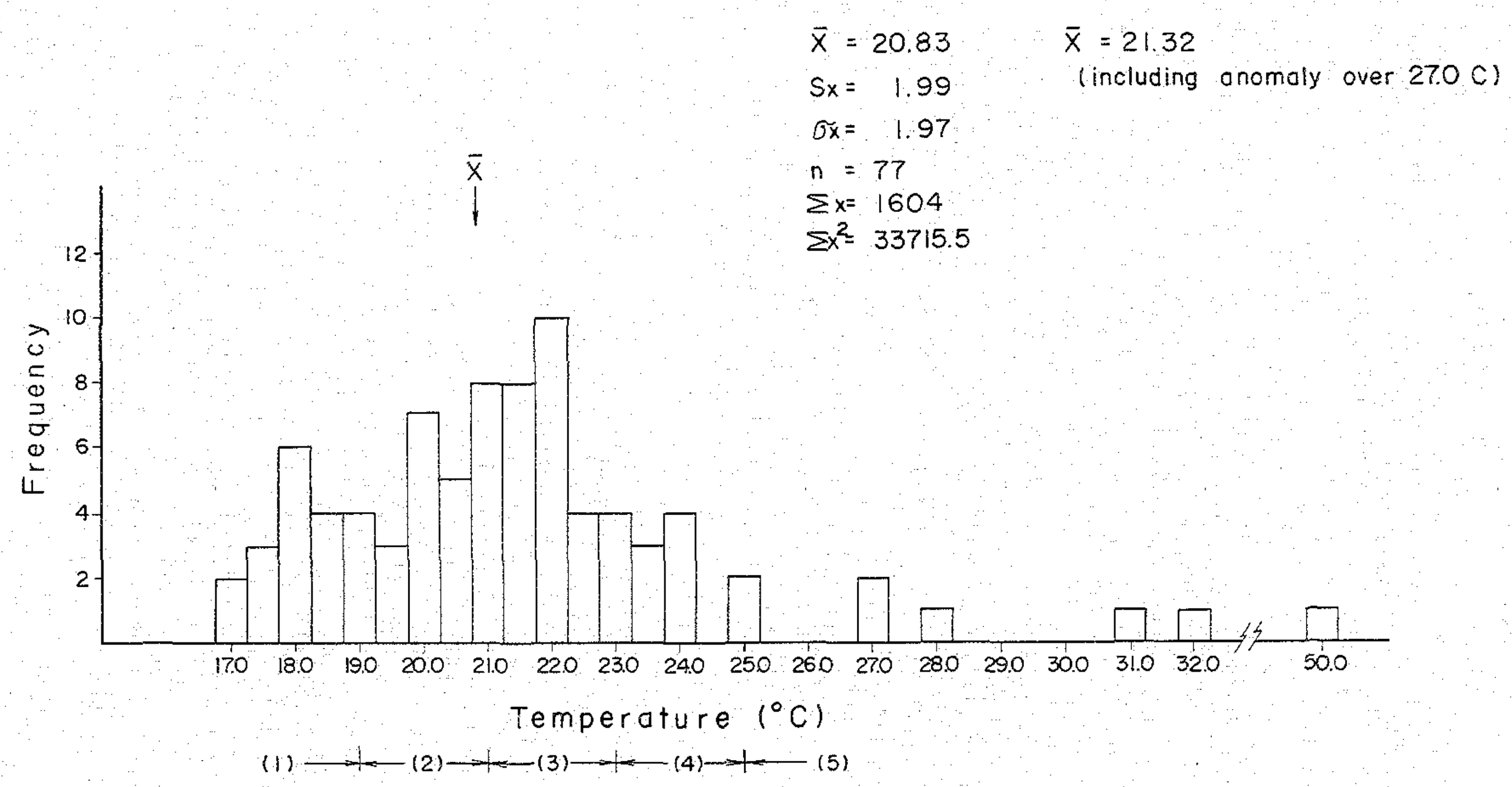

Fig. II–2–4 Frequency of Temperature